Spectroscopically labelled hydroxylamino-triazine (BHT) siderophores toward the quantification of iron(III), vanadium(V) and uranium(VI) hard metal ions

Angelos Amoiridis,[a] Michael Papanikolaou,[a] Chryssoula Drouza,[b] Themistoklis A. Kabanos*[c] and Anastasios D. Keramidas*[a]

[a] *University of Cyprus, Department of Chemistry, 2109, Nicosia, Cyprus. Email: akeramid@ucy.ac.cy*

[b]*Department of Agricultural Sciences, Biotechnology and Food Science, Cyprus University of Technology, Limassol 3036, Cyprus. E-mail: chryssoula.drouza@cut.ac.cy*

[c]*Department of Chemistry, Section of Inorganic and Analytical Chemistry, University of Ioannina, 45110 Ioannina, Greece: E-mail: tkampano@uoi.gr*

Contents **Pages**

Supporting Information

Materials and Methods. All chemicals and solvents were purchased from Merck. Microanalyses for C, H, and N were performed using a Euro-Vector EA3000 CHN elemental analyzer. FT-IR transmission spectra of the compounds were acquired using a Shimadzu IR Spirit model spectrophotometer. The UV-vis measurements were recorded on a Shimadzu UV-Vis spectrophotometer Model UV-2600i, equipped with a CCD array, operating in the range 200 to 900 nm. Merck silica gel 60 F254 TLC plates were used for thin layer chromatography.
X-ray Structure Analysis. X-ray diffraction data of single crystals of the complex compounds were collected on a Rigaku XtaLAB Synergy S diffractometer, equipped with a HyPix-6000HE detector utilizing enhanced Cu Ka (λ = 1.5406 Å) X-ray source and graphite radiation monochromator. CrysAlis CCD and CrysAlis RED software were used for data collection and data reduction/cell refinement respectively. Analytical absorption correction was applied using CrysAlis RED software. The structure of the compounds was solved by direct methods and refined by full matrix least squares techniques on F2 by using SHELXT. Special computing molecular graphics incorporated in the OLEX 2.0 interface were used. All the non-H atoms were anisotropically refined. The positions of hydrogen atoms in all structures were calculated from stereochemical considerations and kept fixed isotropic during refinement or found in DF map and refined with isotropic thermal parameters. ORTEP software was used for molecular graphics. Selected crystal data for **1**-**5** are summarized in tables S3, S4 respectively.

NMR Spectroscopy. NMR measurements. All NMR samples were prepared by dissolving each compound in deuteriated solvents at room temperature just prior to NMR spectrometric determinations. NMR spectra were recorded on a Bruker Avance III 500 MHz spectrometer. A 30º-pulse width was applied for both the ^{1}H (SW= 10331 Hz) and ^{13}C NMR (SW= 29762 Hz) measurements, and 2s relaxation delay. A 90º-pulse width and 0.001s relaxation delay were applied for ^{51}V NMR (SW= 50000 Hz) measurements. For 2D {^{1}H} EXSY NMR, the size of the FID was 2K x 256 for F1 (SW= 1150 Hz) and at F2 (SW= 1150) axes respectively while mixing time was set to 0.5s and relaxation delay to 4s. For {^{1}H} COSY NMR, size of the FID was 6K x 128 for F1 (SW= 1202 Hz) and at F2 (SW= 1202) axes respectively. For 2D {^{1}H, ^{13}C} grHSQC NMR, the size of the FID was 1K x 256 for F1 (SW= 27665 Hz) and F2 (SW= 8013 Hz). Data acquisition and processing were accomplished using TopSpin 4.0.6 and MultiSpecNMR 4.0.0 (https://sourceforge.net/projects/multispecnmr/). Standard pulse programs as implemented in TopSpin were used for data acquisition.

Sample Preparation for ^{1}H & ^{51}V NMR measurements. For the NMR titration of **4** with variable $U^{VI}O_2^{2+}$ concentrations, the samples were prepared as follows: *dmso*-d_6 solution at standard ligand concentration (2.27 μmols) was prepared by dissolving 0.0011 g of complex **1** in 0.62 mL of *dmso*-d_6. To this solution, were added 10-110 μL (0.5-5.5 μmols) portions of a $[U^{VI}O_2(NO_3)_2(H_2O)_2]\cdot 4H_2O$ solution in *dmso*-d_6 (0.05 M). The solution was stirred at room temperature for 10 minutes prior to each measurement to assure chemical equilibrium.

Fluorescence studies. All fluorescence measurements were performed on a JASCO FP-8300 instrument using Quartz cells. Parameters used: Excitation and Emission bandwidths were set at 5nm. Response time was at 20 msec the sensitivity of the measurement was set to high and the Number of scans (NS) was one. Blank correction was applied prior to the measurement. The solutions for the fluorescence quenching experiments were prepared by adding 5 μL fractions of the appropriate metal

solution (200 μM) to the ligand solution (10 μM ligand and 40 μM of triethylamine). The final volume of solutions was 1.300 mL. The solvent for all solutions mentioned was a mixture of DMSO 9:1 H_2O. a) NS

Electrochemistry

Cyclic voltammetry (CV) and Square Wave Voltammetry (SWV) experiments were recorded using an CH Instruments Electrochemical Workstation model CHI650E potentiostat/galvanostat. Electrochemical procedures were performed with a three-electrode configuration: Glassy carbon was used as the working electrode, a platinum wire as the auxiliary electrode, and Ag/AgCl (0.20 V vs NHE) as reference. The potential of the reference electrode was measured with ferrocene (0.65 V vs NHE). All the potential values are referred to NHE. The electrochemical measurements were carried out in DMF solutions of But_4NClO_4 (0.1 M) purged with N_2 prior to the measurements at 298 K. Scan rate (ν) of 100 mV s^{-1} was used for cyclic voltammograms. For Square Wave Voltammetry experiments, the Increment was 0.004 V, Amplitude was 0.025 V and the frequency was set at 15 Hz.

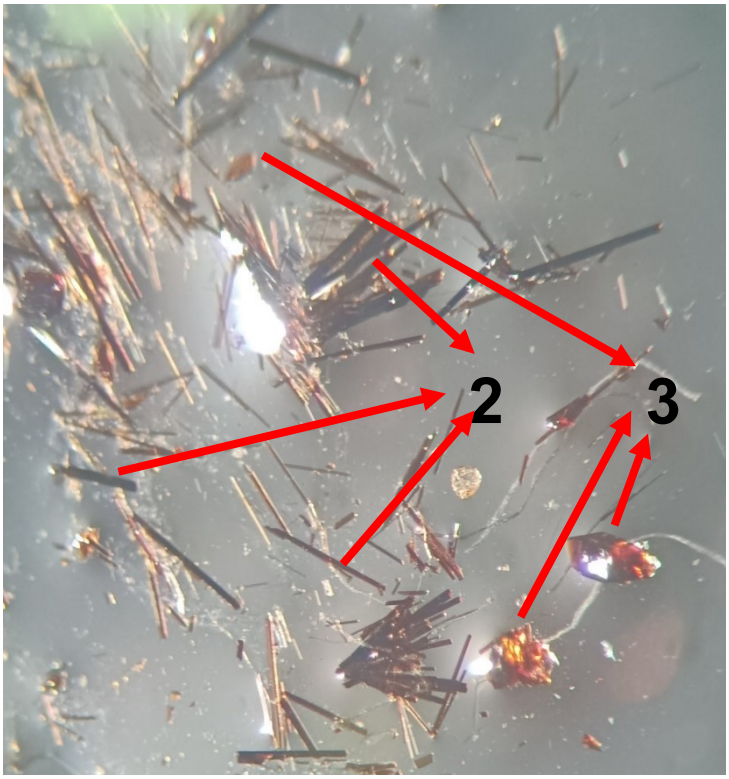

Figure S1. Co-crystalization of complexes **2** and **3** under microscope. Complex **2** crystalizes as rod-like crystals while complex **3** as blocks.

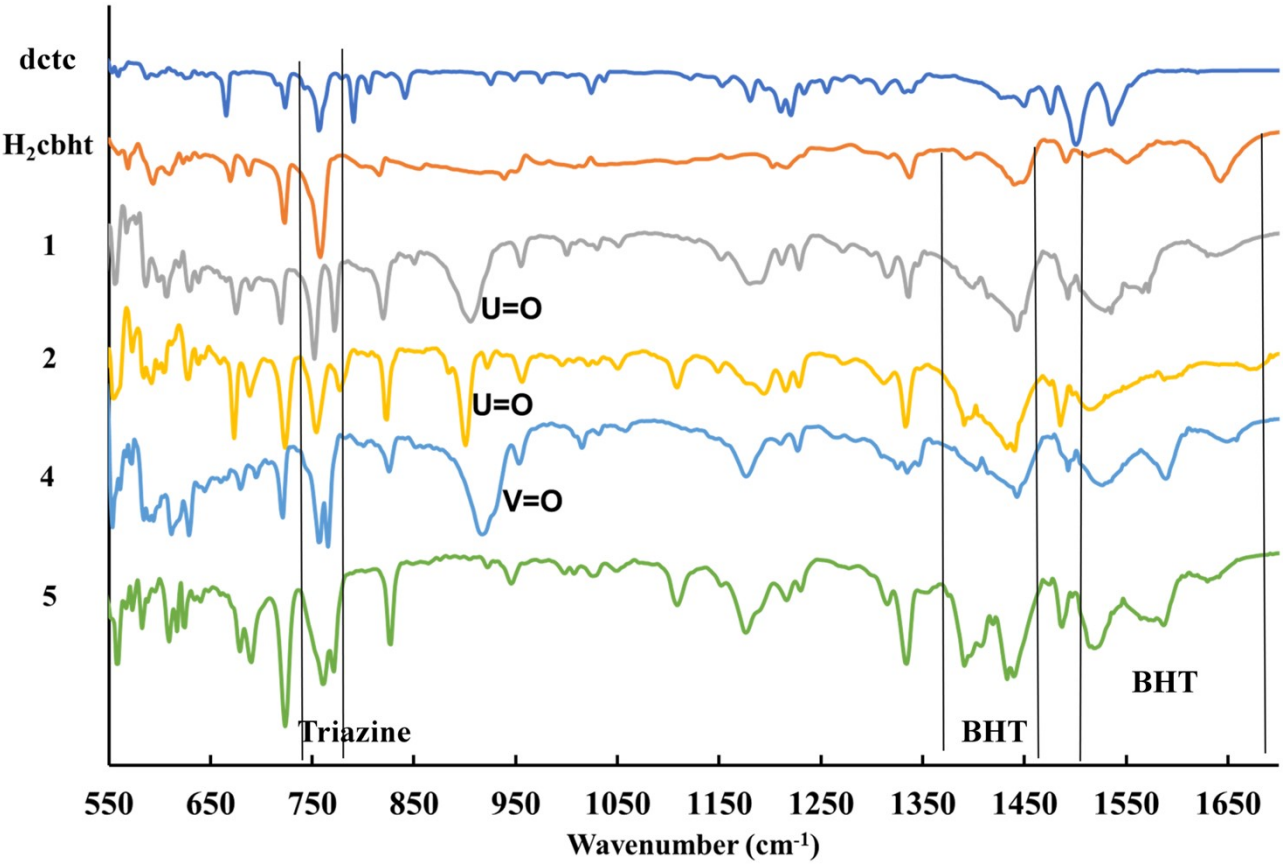

Figure S2. Infra red spectra of dctc, H_2cbht and **1**, **2**, **4** and **5** and assignments.

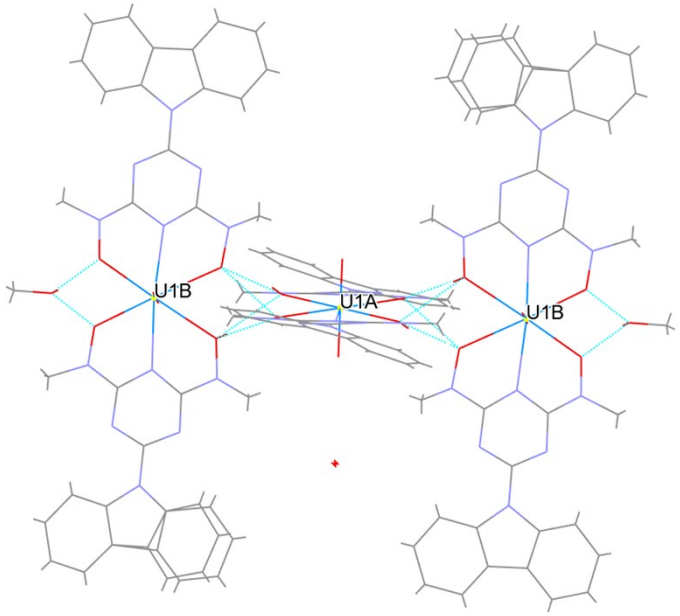

Figure S3. Wireframe drawing of the crystal structure of **2**.

NMR

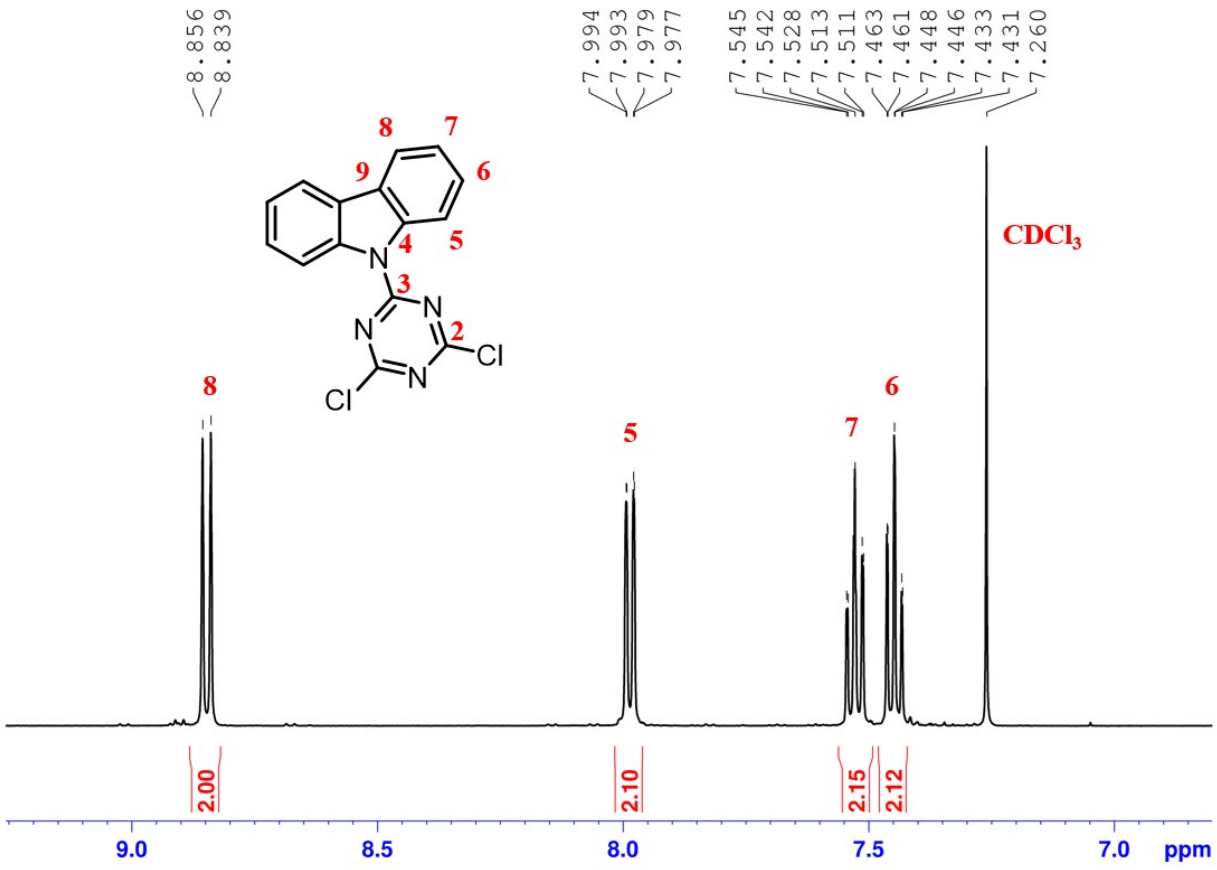

Figure S4: ^{1}H NMR spectrum of dctc in $CDCl_3$, 500 MHz, 20^{o}C.

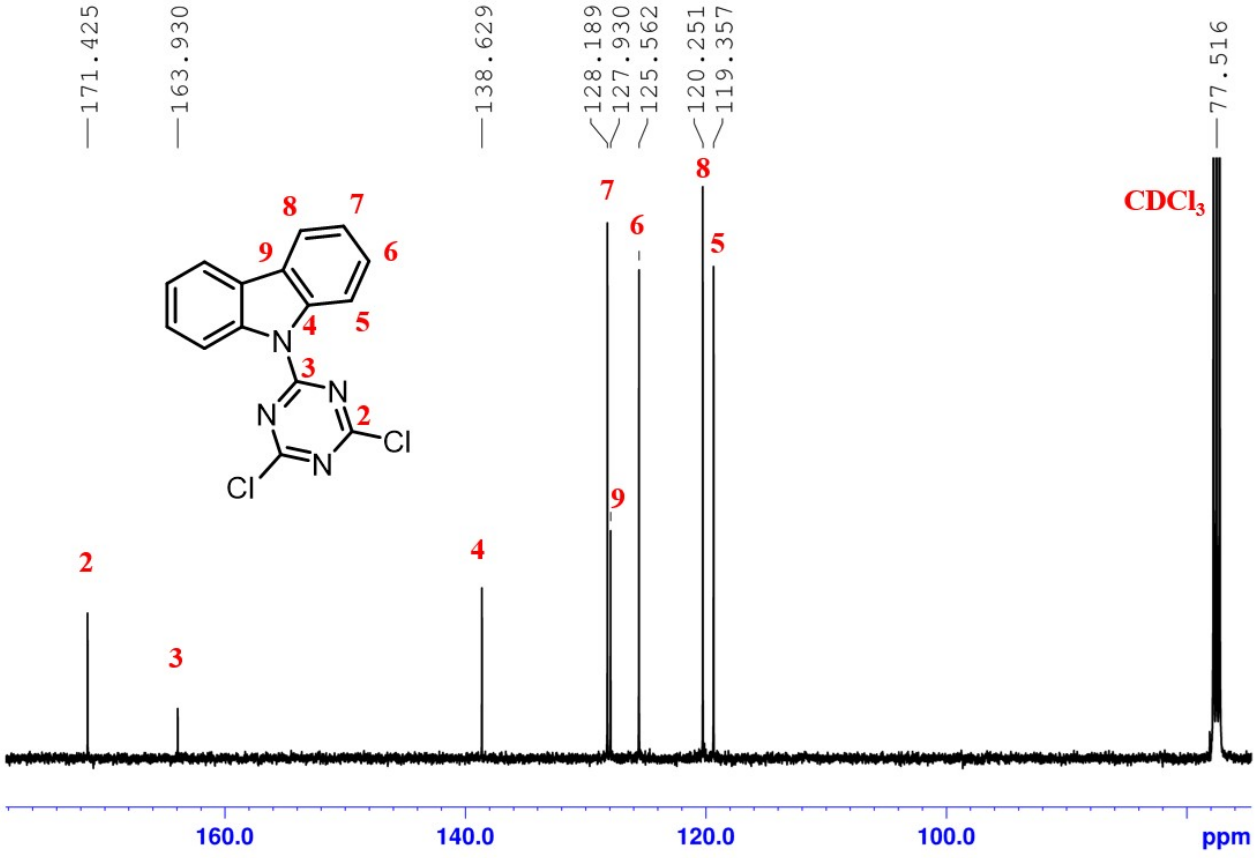

Figure S5: ^{13}C NMR spectrum of dctc in $CDCl_3$, 126 MHz, 20°C.

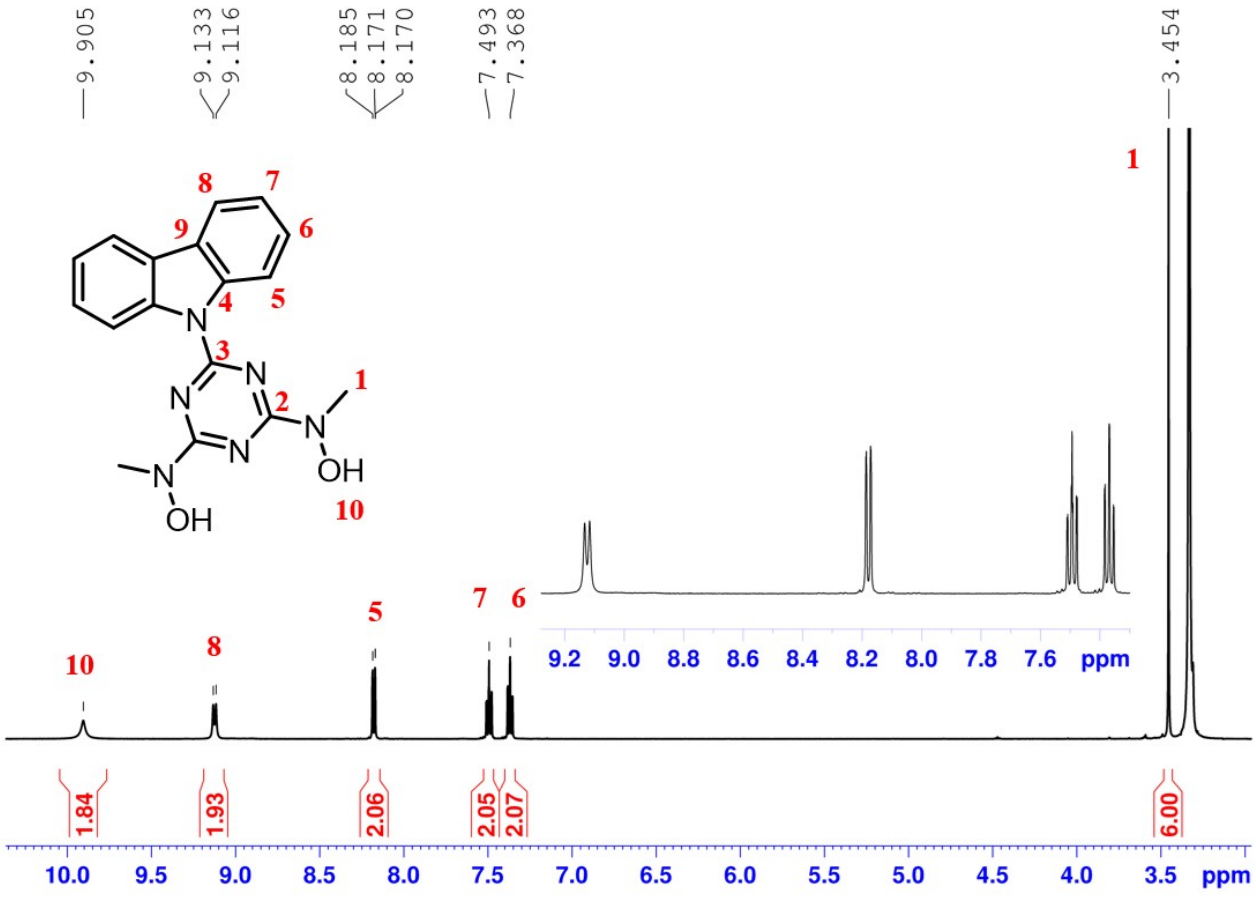

Figure S6: ^{1}H NMR spectrum of H_2cbht in DMSO-d_6, 500 MHz, 20°C.

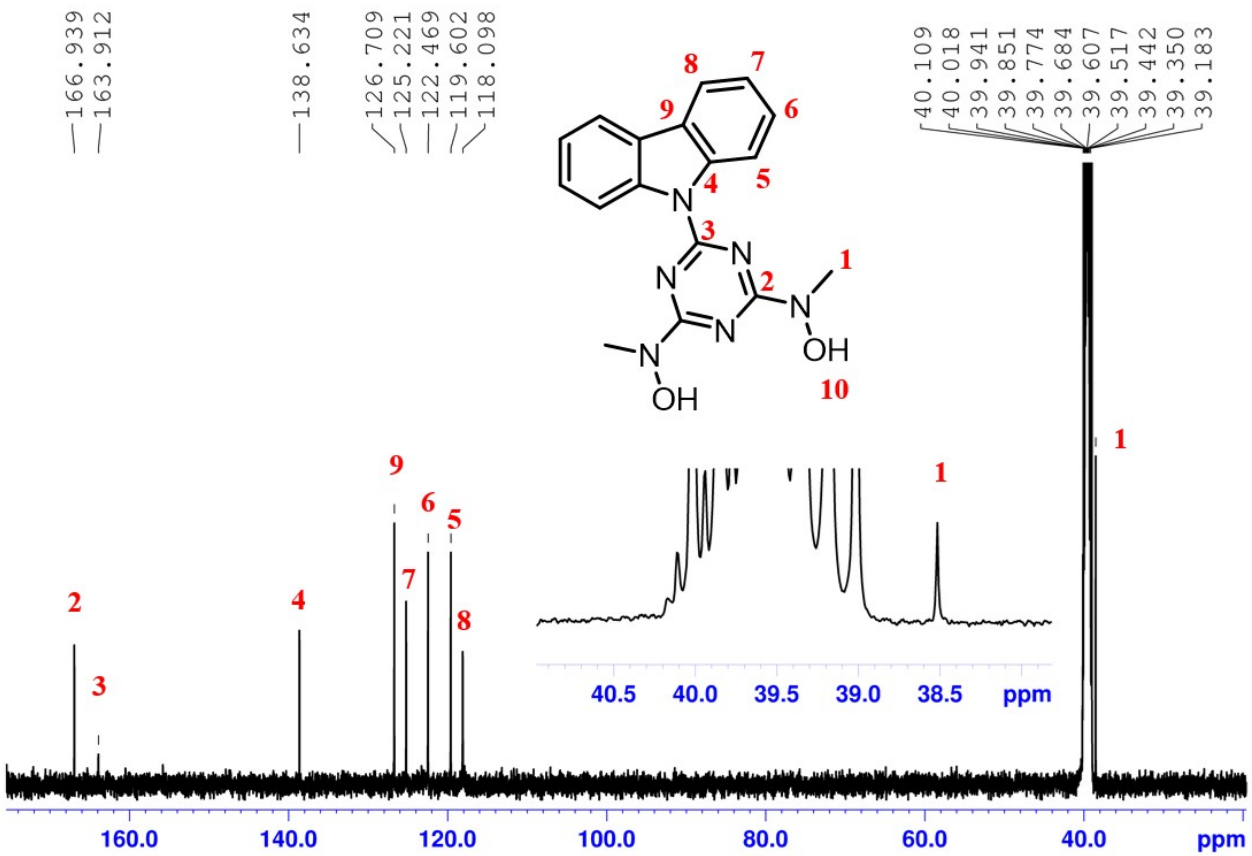

Figure S7: ^{13}C NMR spectrum of H_2cbht in DMSO-d_6, 126 MHz, 20°C.

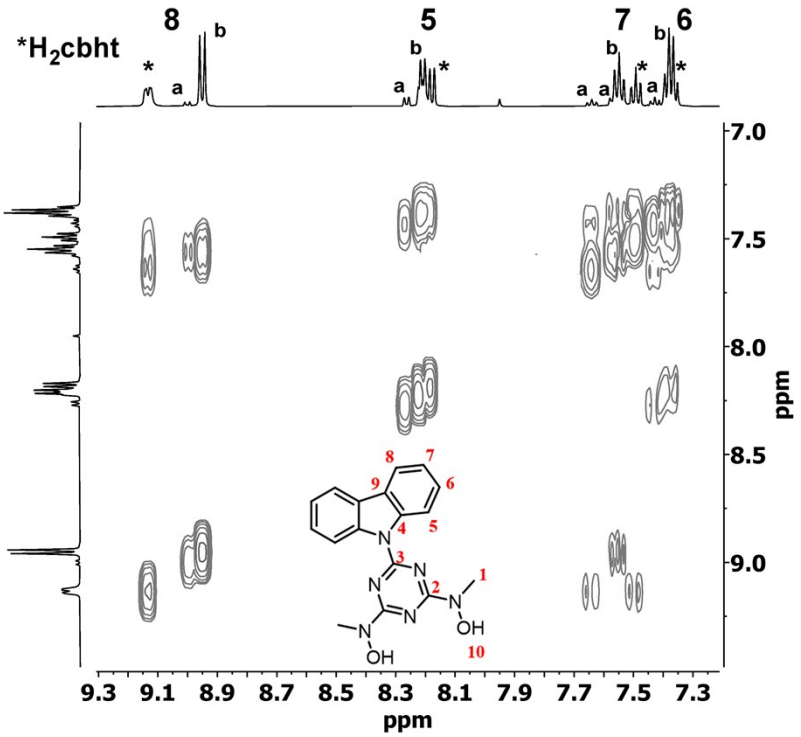

Figure S8. 2D {^{1}H} grCOSY spectrum of the aromatic region of a dmso-d_6 solution of a solution of **1** (x mM), H_2cbht (x mM) and Et_3N (x mM). (a=carbazole protons on cbht^{2-} containing sp^3 N atoms, b=carbazole protons on cbht^{2-} containing only sp^2 N atoms)

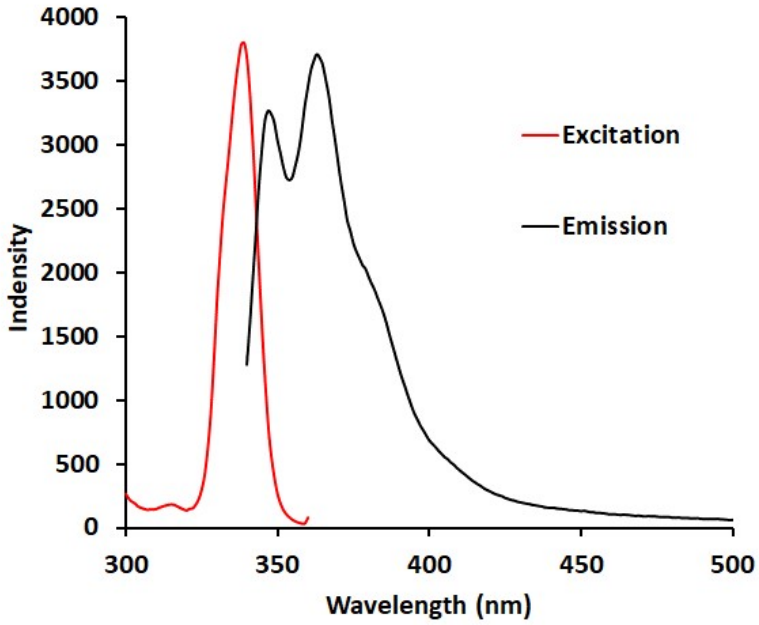

Figure S9. Excitation and emission spectrum of 1.00 mM M of H_2cbht in dmso.

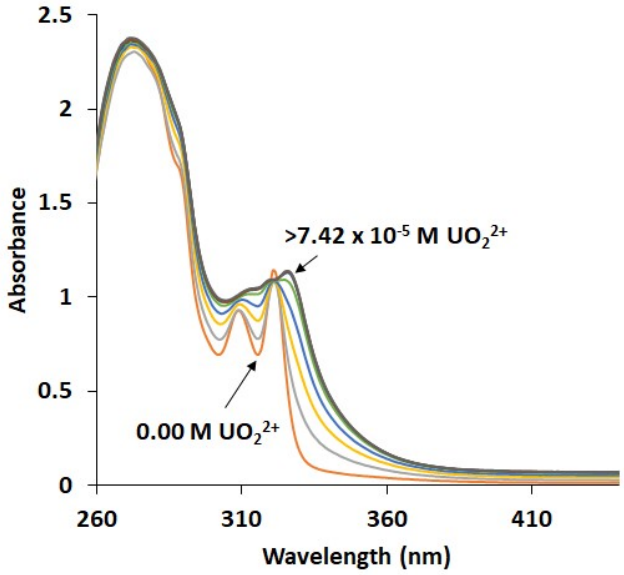

Figure S10. UV-vis spectra of 7.42 x 10^{-5} M of H_2cbht and 27.7 x 10^{-5} M of Et_3N in dmso titrated by $U^{VI}O(NO_3)_2$ in dmso. In each spectrum, $U^{VI}O_2^{2+}$ is added in order the concentration of the metal ion to be increased by 1.58 x 10^{-5} M.

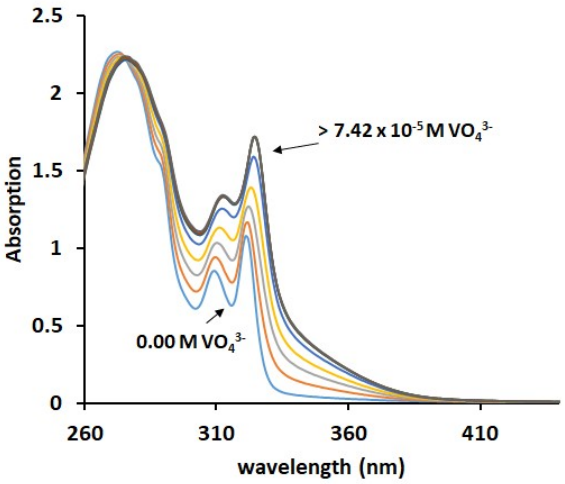

Figure S11. UV-vis spectra of 7.42 x 10^{-5} M of H_2cbht and 27.7 x 10^{-5} M of Et_3N in dmso titrated by $NaV^{V}O_3$ in H_2O. In each spectrum, $V^{V}O_4^{3-}$ is added in order the concentration of the metal ion to be increased by 1.58 x 10^{-5} M.

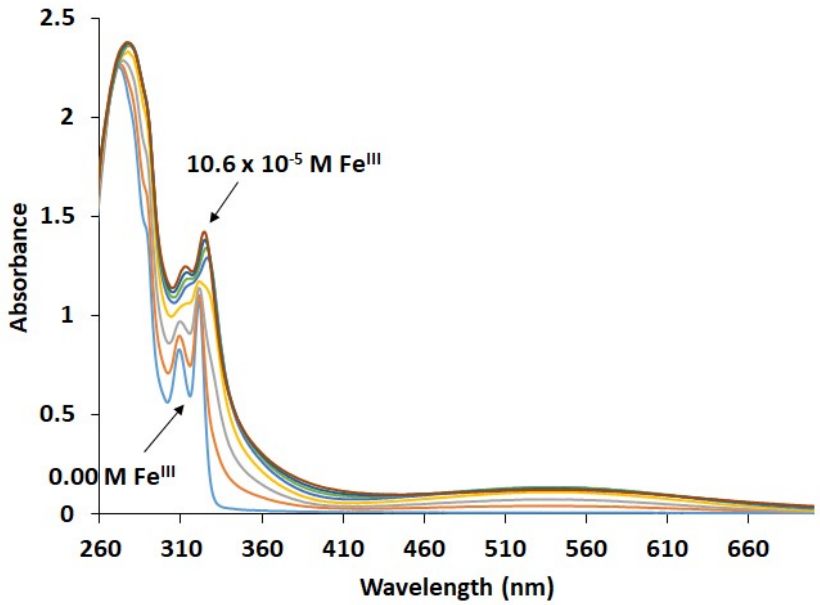

Figure S12. UV-vis spectra of 7.42 x 10^{-5} M of H_2cbht and 27.7 x 10^{-5} M of Et_3N in dmso titrated by $Fe^{III}(NO_3)_3$ in dmso. In each spectrum, Fe^{III} is added in order the concentration of the metal ion to be increased by 1.58 x 10^{-5} M.

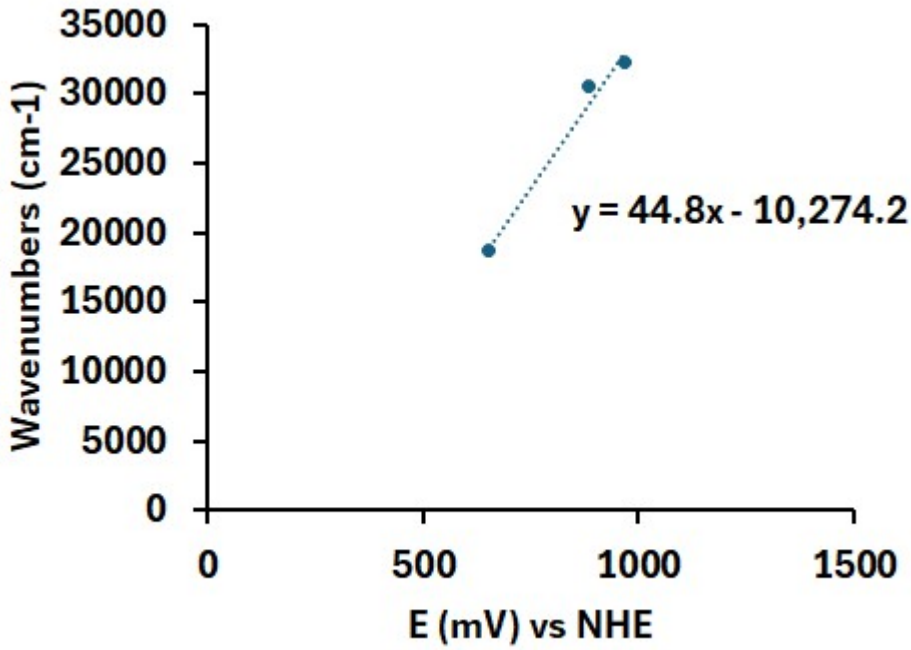

Figure S13. Plot of the energy of the LMCT peaks *vs* the potential of the ligand center oxidation for complexes **1**, **4** and **5**.

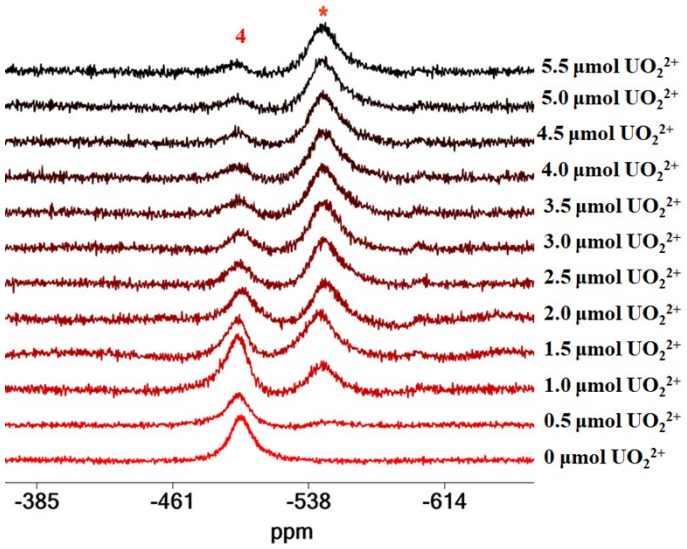

Figure S14. ^{51}V NMR spectra of solutions (DMSO-d_6) that contain **4** (2.27 µmols) and $U^{VI}O_2$ (0-5.5 µmols). With * the peak from inorganic vanadates.

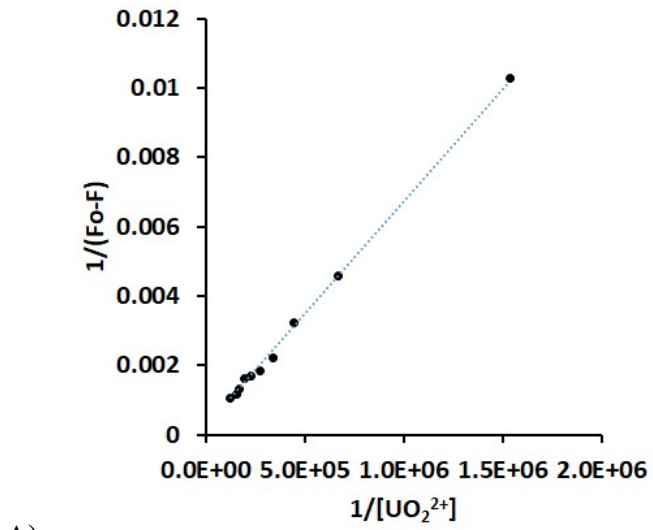

A)

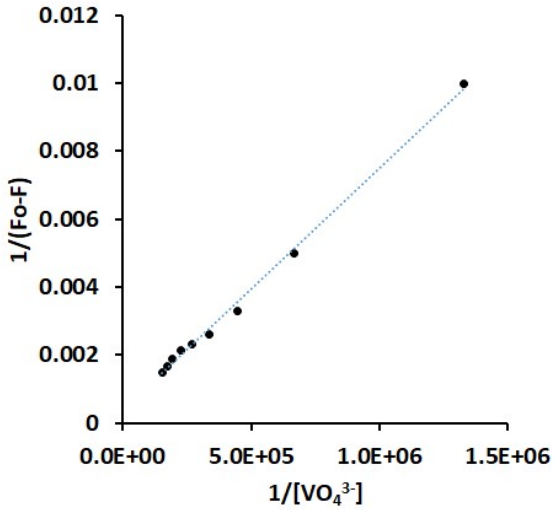

B)

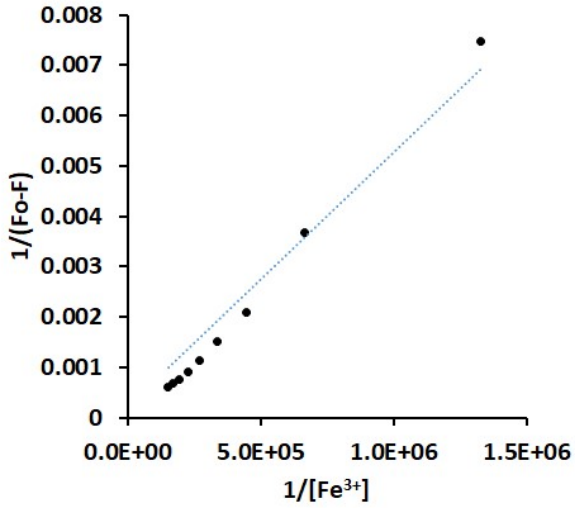

C)

Figure S15.A) Benesi-Hildebrand plot of $U^{V}O_2^{2+}$ added in a DMSO 9:1 H_2O solution of H_2cbht (3.74 x 10^{-5} M) and Et_3N (14.8 x 10^{-5} M), B) Benesi-Hildebrand plot of VO_4^{3-} added in a DMSO 9:1 H_2O solution of H_2cbht (3.74 x 10^{-5} M) and Et_3N (14.8 x 10^{-5} M), C) Benesi-Hildebrand plot of Fe^{3+} added in a DMSO 9:1 H_2O solution of H_2cbht (3.74 x 10^{-5} M) and Et_3N (14.8 x 10^{-5} M).

Table S1: Crystal Data and Structure Refinement for the compounds 1 and 2.

Parameter	1	2	3
Empirical formula	$C_{21}H_{25}N_7O_6U$	$C_{80}H_{79.50}N_{18}O_{11.75}PU_{1.50}$	$C_{122}H_{110}N_{26}O_{16}P_2U_3$
Formula weight	709.51	1869.13	2972.38
Temperature/K	293(2)	150(2) K	150.0(1)
Crystal system	triclinic	Monoclinic	triclinic
Space group	P-1	P 21/n	P-1
a/Å	10.39940(10)	24.7499(9)	13.5096(2)
b/Å	10.40700(10)	34.5643(3)	13.6013(2)
c/Å	11.93030(10)	13.4753(5)	17.1971(2)
α/°	109.3150(10)	90	99.7750(10)
β/°	93.6850(10)	136.637(7)	103.0330(10)
γ/°	94.3070(10)	90	106.2090(10)
Volume/Å^3	1209.60(2)	7915.1(8)	2863.23(7)
Z	2	4	1
ρ_{calc}g/cm^3	1.948	1.569	1.724
μ/mm^{-1}	19.335	9.390	12.719
F(000)	680.0	3730	1458.0
Crystal size/mm^3	0.23 × 0.12 × 0.04	0.087 x 0.061 x 0.042	0.08 × 0.05 × 0.05
Radiation	Cu Kα (λ = 1.54184)	Cu Kα (λ = 1.54184)	Cu Kα (λ = 1.54184)
2Θ range for data collection/°	7.888 to 153.61	2.898 to 77.431	5.446 to 154.51
Index ranges	-12 ≤ h ≤ 12, -13 ≤ k ≤ 13, -14 ≤ l ≤ 15	-31≤ h ≤31, -43 ≤k ≤16, -17 ≤ l ≤16	-17 ≤ h ≤ 16, -16 ≤ k ≤ 14, -21 ≤ l ≤ 21
Reflections collected	43635	56751	37937
Independent reflections	4883 [R_{int} = 0.0460, R_{sigma} = 0.0185]	16196 [R(int) = 0.0444]	11683 [R_{int} = 0.0404, R_{sigma} = 0.0392]
Data/restraints/parameters	4883/0/322	16196 / 4 / 1055	11683/0/797
Goodness-of-fit on F^2	1.111	1.037	1.057
Final R indexes [I>=2σ (I)]	R_1 = 0.0161, wR_2 = 0.0406	R1 = 0.0308, wR2 = 0.0780	R_1 = 0.0315, wR_2 = 0.0751
Final R indexes [all data]	R_1 = 0.0162, wR_2 = 0.0407	R1 = 0.0368, wR2 = 0.0805	R_1 = 0.0349, wR_2 = 0.0767
Largest diff. peak/hole / e Å^{-3}	0.53/-0.95	1.202/-1.779	2.12/-1.81

[a] $R1 = \Sigma||F_o| - |F_c||/\Sigma|F_o|$. [b] $wR2 = \{\Sigma[w(F_o^2 - F_c^2)^2]/\Sigma[w(F_o^2)_2]\}1/2$, where $w = 1/[\sigma^2(F_o^2)+(aP)^2+bP]$, $P = (F_o^2+2F_c^2)/3$. [c] $GoF = \{\Sigma[w(F_o^2-F_c^2)_2]/(n-p)\}^{1/2}$, where n = number of reflections and p is the total number of parameters refined.

Table S2: Crystal Data and Structure Refinement for the compounds **3** and 4.

Parameter	**4**	**5**
Empirical formula	$C_{17}H_{20}N_6NaO_7V$	$C_{58}H_{63}FeN_{12}O_{13}P$
Formula weight	494.32	1223.02
Temperature/K	149.96(10)	155.0(2)
Crystal system	triclinic	triclinic
Space group	P-1	P-1
a/Å	7.03000(10)	14.2496(7)
b/Å	10.52220(10)	15.3470(7)
c/Å	14.68810(10)	16.5555(5)
α/°	79.5520(10)	101.555(3)
β/°	81.2120(10)	108.396(4)
γ/°	71.4500(10)	113.274(4)
Volume/Å^3	1007.69(2)	2928.4(2)
Z	2	2
ρ_{calc}g/cm^3	1.626	1.387
μ/mm^{-1}	4.832	2.948
F(000)	508.0	1280.0
Crystal size/mm^3	0.235 × 0.114 × 0.075	0.105 × 0.058 × 0.025
Radiation	CuKα (λ = 1.54184)	Cu Kα (λ = 1.54184)
2Θ range for data collection/°	6.15 to 153.436	6.064 to 153.28
Index ranges	-8 ≤ h ≤ 8, -12 ≤ k ≤ 13, -17 ≤ l ≤ 18	-17 ≤ h ≤ 17, -19 ≤ k ≤ 19, -20 ≤ l ≤ 18
Reflections collected	37003	37055
Independent reflections	4044 [R_{int} = 0.0331, R_{sigma} = 0.0137]	11912 [R_{int} = 0.0815, R_{sigma} = 0.0825]
Data/restraints/parameters	4044/0/298	11912/2/797
Goodness-of-fit on F^2	1.079	1.027
Final R indexes [I>=2σ (I)]	R_1 = 0.0286, wR_2 = 0.0812	R_1 = 0.0693, wR_2 = 0.1722
Final R indexes [all data]	R_1 = 0.0288, wR_2 = 0.0814	R_1 = 0.1174, wR_2 = 0.2028
Largest diff. peak/hole / e Å^{-3}	0.511/-0.456	0.95/-0.78

[a] $R1 = \Sigma||F_o| - |F_c||/\Sigma|F_o|$. [b] $wR2 = \{\Sigma[w(F_o^2 - F_c^2)^2]/\Sigma[w(F_o^2)_2]\}1/2$, where $w = 1/[\sigma^2(F_o^2)+(aP)^2+bP]$, $P = (F_o^2+2F_c^2)/3$. [c] $GoF = \{\Sigma[w(F_o^2-F_c^2)_2]/(n-p)\}^{1/2}$, where n = number of reflections and p is the total number of parameters refined.

Table S3: Interatomic Distances (Å) and Angles (deg) Relevant to the U^{VI}, Fe^{III} coordination Sphere.

Parameter	**2**			**5**	
	U_A	**U_B**		**Hcbht$^-$**	**Hcbht$^-$ '**
		Hcbht$^-$	**Hcbht$^-$ '**		
M-O1	1.782(3)	1.780(3)		2.029(3)	2.043(3)
M-O2	1.782(3)	1.782(3)		2.119(3)	2.114(3)
M-O3	2.476(3)	2.356(3)	2.621(3)	-	-
M-O4	2.480(3)	2.584(3)	2.324(3)	-	-
M-N3	2.531(4)	2.551(3)	2.551(3)	1.980(3)	1.997(4)
O1-M-O3	88.56(13)	92.43(13)	90.23(11)	-	-
O1-M-O4	86.63(11)	87.03(11)	92.72(12)	-	-
O1-M-N3	94.11(12)	90.61(12)	89.50(12)	75.54(12)	75.19(13)
O2-M-O3	91.39(11)	91.61(12)	85.66(11)		
O2-M-O4	86.63(11)	88.83(11)	91.33(12)	-	-
O2-M-N3	94.11(12)	89.14(12)	90.24(12)	73.52(11)	73.68(12)
O2-M-O1	180.0	175.30(12)		148.24(12)	148.58(11)
O3-M-O4	120.41(8)	120.65(9)	120.48(9)	-	-
N3-M-O3	60.70(9)	62.08(10)	57.88(9)	-	-
N3-M-O4	60.50(9)	58.59(9)	62.72(10)	-	-

Table S4: Interatomic Distances (Å) and Angles (deg) Relevant to the U^{VI}, V^{V}, coordination Sphere.

Parameter	1	4
M-O1	1.780(2)	1.6318(12)
M-O2	1.776(2)	1.6313(13)
M-O3	2.415(0)	2.0140(11)
M-O4	2.299(2)	1.9706(12)
M-O5	2.400(2)	-
M-O6	2.381(2)	-
M-N3	2.433(2)	1.9839(13)
O1-M-O3	87.28(8)	98.74(6)
O1-M-O6	87.43(9)	-
O1-M-O4	91.85(9)	101.15(6)
O1-M-O5	89.21(9)	-
O1-M-N3	90.80(9)	122.16(7)
O2-M-O3	91.08(8)	97.30(6)
O2-M-O6	88.25(9)	-
O2-M-O4	92.38(9)	98.96(6)
O2-M-O5	90.80(9)	-
O2-M-N3	92.07(9)	128.96(7)
O2-M-O1	175.63(9)	108.83(8)
O3-M-O4	126.76(7)	148.59(5)
N3-M-O3	63.15(7)	74.29(5)
N3-M-O6	139.55(7)	-
N3-M-O4	63.64(7)	74.57(5)
N3-M-O5	138.73(8)	-

Parameter	3	
	U_1	U_2
U-O1	1.777(3)	1.781(3) [a]
U-O2	1.793(3)	1.781(3) [a]
U-O3	2.309(3)	-
U-O4	2.319(3)	-
U-O3’	2.438(3)	2.466(3)
U-O4’	2.454(3)	2.503(3)
U-N3	2.430(4)	2.530(3) [c]
O1-U-O3	90.33(15)	91.15(12) [a,b]
O1-U-O4	88.65(15)	86.21(12) [a,b]
O1-U-N3	84.59(14)	87.83(13) [a,c]
O2-U-O3	89.84(14)	88.85(12) [a,b]
O2-U-O4	90.95(14)	93.79(12) [a,b]
O2-U-N3	95.15(14)	92.17(13) [a,c]
O2-U-O1	179.59(16)	180.00(19) [a]
O3-U-O4	126.96(12)	121.06(9) [b]
N3-U-O3	63.39(12)	60.77(10) [b,c]
N3-U-O4	63.73(12)	60.52(10) [b,c]
U1-O3’-U2	109.87(11)	
U1-O4’-U2	108.14(10)	

a For Complex 3, atom U2, O1 & O2 on table are the O5 atom from crystal structure. **b** For Complex 3 and angles around U2 atom, O3 & O4 from table are referred to O3’ & O4’ from crystal structure respectively. **c** For Complex 3, atom U2, atom N3 on table is atom N3’ from crystal structure.

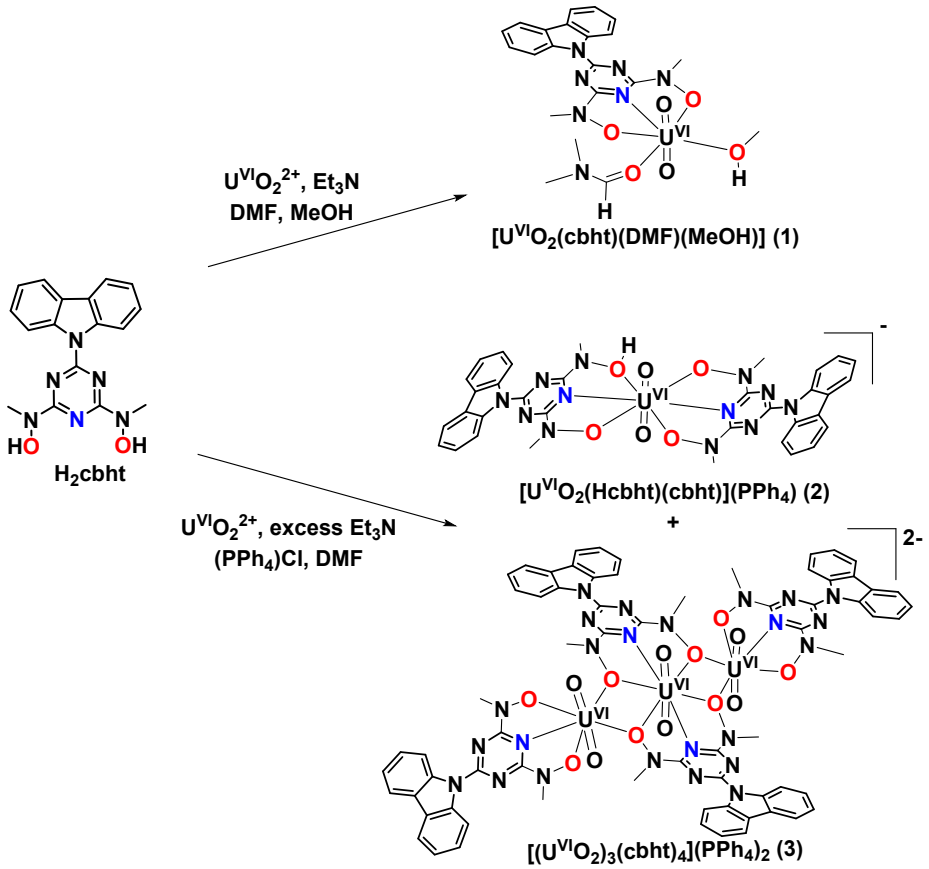

Scheme S1 Synthesis of the complexes of $U^{VI}O_2^{2+}$with H_2cbht.

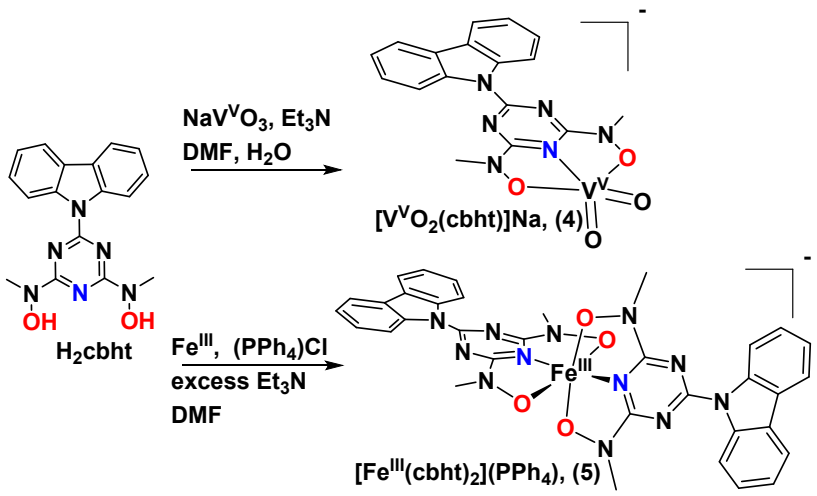

Scheme S2 Synthesis of the complexes of $V^{V}O_2^{+}$ and Fe^{III} with H_2cbht.